Modeling the 2012 Wharton Basin Earthquakes off-Sumatra; Complete Lithospheric Failure

Shengji Wei, Don Helmberger and Jean-Philippe Avouac
Seismological Labatory, Division of Geological and Planetary Sciences, Caltech, Pasadena

A sequence of large strike-slip earthquakes occurred about 200km west of Aceh beneath the Wharton Basin which is sandwiched between the Ninety-East Ridge and the Sunda Trench. First reports indicate that this intraplate event was extremely complex involving three to four subevents MW>8 with a maze of aftershocks spread across the entire basin. Here we develop a kinematic slip model of the sequence to better understand the northeastern edge of the Australia plate tectonics encountering compression and subduction. Without near field geodetic data, we had to develop hybrid Green's Functions to model the regional oceanic-continental surface wave observations. These included 4 Indian Oceanic Island stations and 7 mixed-paths to the north and east. We perform a joint inversion of these regional observations along with teleseismic body waveform data to recover the rupture details. We employed a combination of simulated-annealing and grid-search techniques to develop a finite rupture model involving three interacting fault planes striking 289° (F1), 20° (F2) and 310° (F3) and dipping 89°, 74° and 60°, respectively. The modeled rupture consists of cascade of high stress drop asperities (with stress drop between 10 and 30MPa). The timing of those ruptures is consistent with a slow initiation followed by a relatively smooth propagation of a rupture front from one fault to the other (F1, F2 and F3 in sequence) with rupture velocities of 2~2.5km/s. The whole process generated a 200s long moment rate function with multiple peaks and an apparent E-W directivity which is actually the result of interferences of waves generated by near simultaneous rupture of various asperities. The asperities ruptured during the main shock and the Mw8.2 aftershock which occurred 2 hours later, span a depth range between 0 and 50km. This suggests that the earthquake sequence, which is part of broad left-lateral shear zone between the Australia and India plates, ruptured the whole oceanic lithosphere. The incremental strain due to the earthquake sequence is consistent with this interpretation. The earthquake sequence reactivated existing fracture zones of the Fossil Wharton Ridge to the south and was probably triggered by unclamping due to the great Sumatra earthquake of 2004.

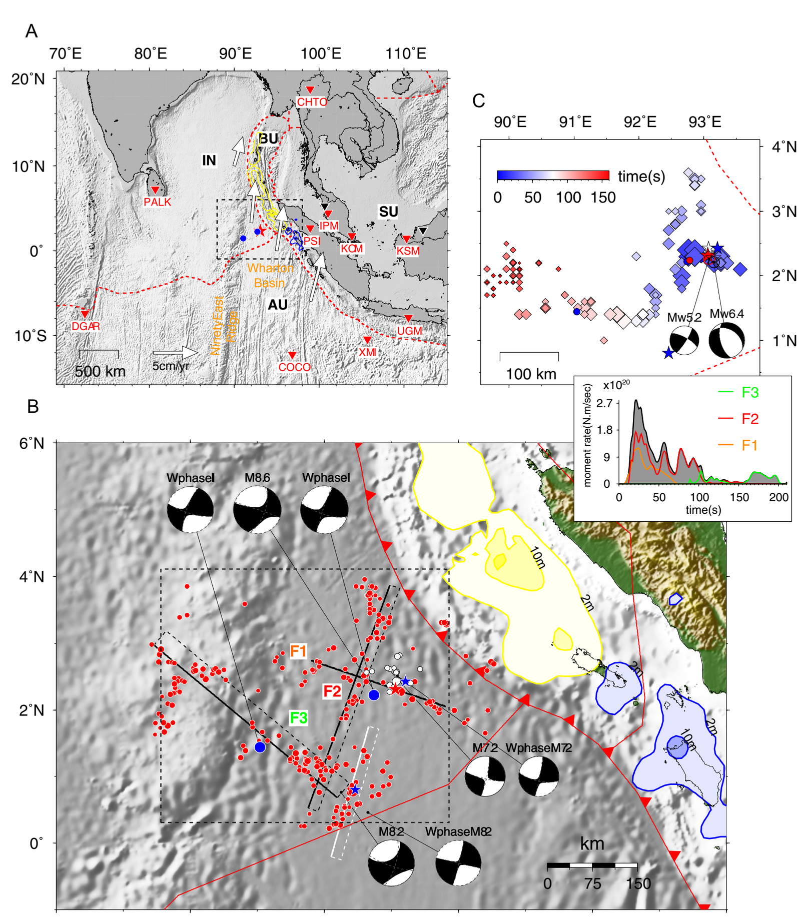

Figure 1

Figure 1. Tectonic setting and overview
(A). Tectonic setting in Sunda-Sumatra region. The arrows indicate the plate motion between Australian Plate (AU) and Sunda Plate (SU), Indian Plate (IN) and Sunda Plate. Red triangles are the regional stations used in study of the main shock, the two black triangles are additional stations used for the M8.2 aftershock. Yellow and blue contours show the slip model of 2004 Mw9.2 and 2005 Mw8.6 earthquakes, respectively. Red dashed lines are the plate boundaries defined in (Bird 2003). (B). Map view of the fault geometry consists of three fault segments (F1, F2 and F3). The white rectangle is the map view of the fault segment used for inverting the Mw8.2 aftershock. The beach balls are the GCMT and W-phase solutions for the main shock, Mw8.2 aftershock and Mw7.2 foreshock. The blue and red starts indicate the NEIC epicenter of these events. The W-phase solution for the main shock includes two point source (blue dots), with moment magnitude of 8.5 (I) and 8.3 (II). The red dots are the aftershocks in the first two months and the white dots are the seismicity in the first 4 months before the main shock, locations are obtained from GFZ catalog. Yellow and blue contours are the same as in A. The inset shows the moment-rate function of the main event along with the contribution of each segment. C. Beach balls display the mechanisms of the main shock, initiation with the Mw5.2 event corresponding to the first 5s and the Mw6.4 with the first 12s. The back projection results are shown as diamonds ((Meng et al. 2012)

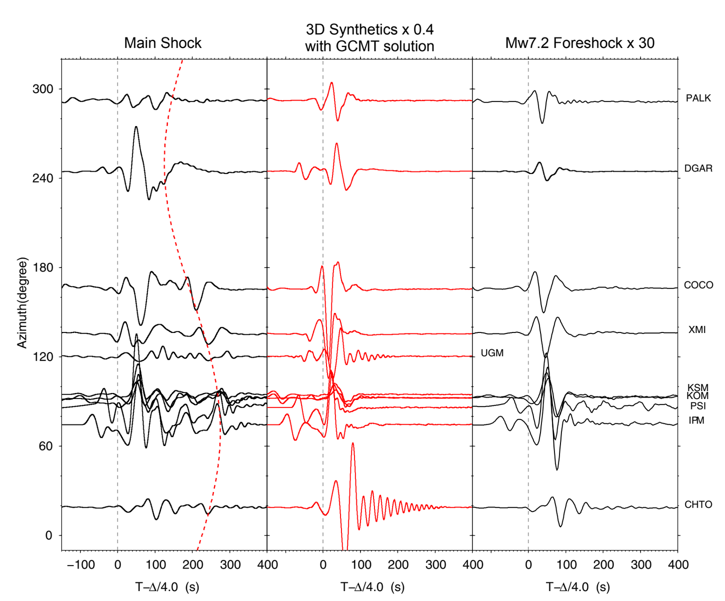

Figure 2

Figure 2. Regional vertical component for mainshock and foreshock
Regional velocity record (vertical component) of the main shock and foreshock and SEM synthetics generated from a 3D model (red) of the main shock downloaded from http://global.shakemovie.princeton.edu/ as shown in the middle column. All the waveforms are filtered to 50s and longer using a 4th order 1 pass Butterworth filter. Note that the true amplitude is plotted with different scaling factor for 3D synthetics (0.4) and foreshock (30). The red dashed line in the data is a theoretical prediction assuming a second point source located 300km to the southwest (azimuth 250°) of the epicenter assuming that the seismic wave travels at a speed of 4.0km/s.

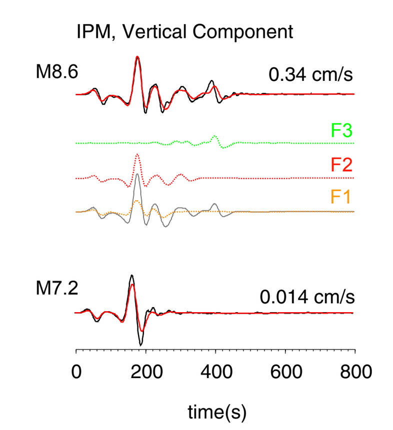

Figure 3

Figure 3. Example fits for IPM
Example waveform fits of the vertical component of station IPM for the main shock and the foreshock. The maximum amplitude of data is shown at the end of the record. The synthetic (gray) for the main shock is decomposed into the contribution from F1 (brown) , F2 (red) and F3 (green). Note the synthetic for the foreshock is generated by the GCMT solution. All the synthetics are filtered to 50s and longer using the same filter as in Fig.2.

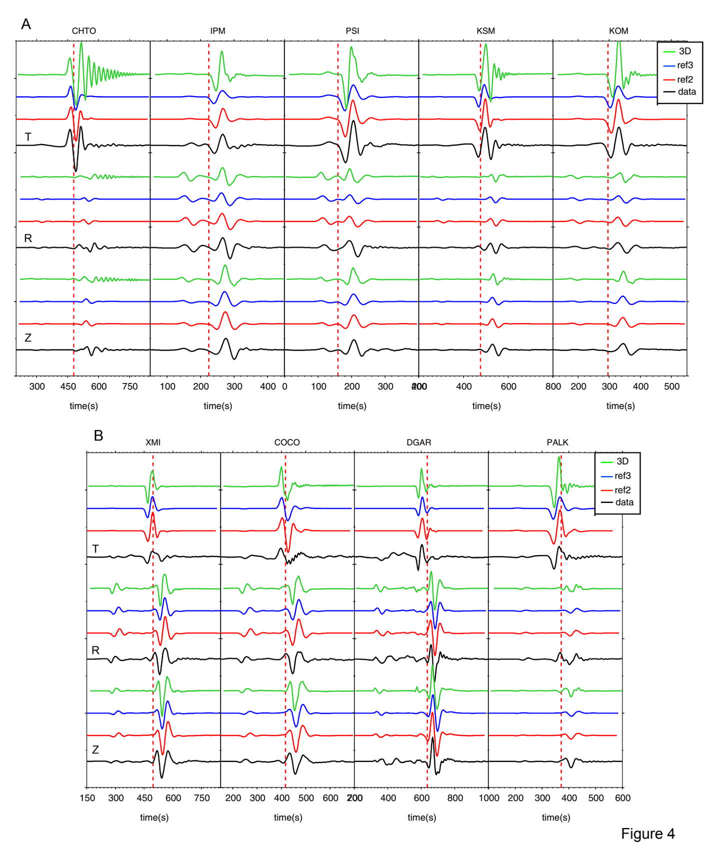

Figure 4

Figure 4. Regional waveforms of the foreshock, include, data, synthetics of ref2, ref3 and 3D model
Regional waveform of the foreshock includes data (black), synthetics generated by 1D velocity models (ref2/red and ref3/blue) and 3D velocity model (green). Stations are divided into two groups according to paths as displayed in A (ref2, red) and B(ref3, blue). The true amplitude of seismograms are plotted with scaling factors for different stations for better display purposes. Seismograms are all filtered to 50s and longer using the same filter as in Fig.2.

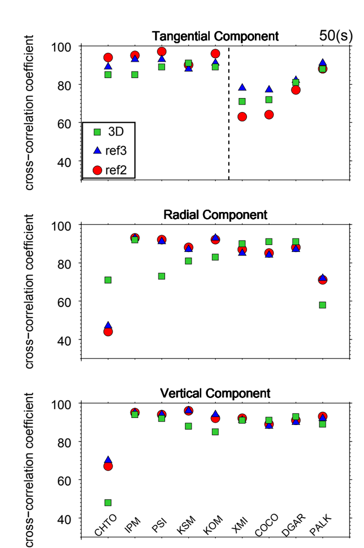

Figure 5

Figure 5. Cross-correlation coefficients between data and synthetics for the foreshock calibration.
Summary of waveform cross-correlation coefficients (CCs) between the data and 1D synthetics (red/ref2, blue/ref3), and 3D synthetics (green). CCs for vertical, radial and tangential are displayed from bottom to top. Note the ref2 model can fit the continental paths better while the ref3 model favors the oceanic paths, separated by the dashed line.

Figure 6

Figure 6. CAP inversion result
Cut-And-Paste (CAP) inversion result for the foreshock. A grid search for the best depth with intervals of 5km is applied; here the waveform fits for the best depth (15km) are shown. Station names are indicated at the beginning of the record along with distance in km (upper) and azimuth in degree (lower). The first number below each waveform pair is time shifts needed to aligned synthetic and data, and the second number is waveform cross-correlation coefficient in percentage. Positive time shift means the velocity model is too fast. The red beach ball at the top shows the lower hemisphere projection of the mechanism (10°/80°/-26°/7.24 for strike/dip/rake/Mw) and the dots in it indicate station projections on the lower hemisphere, each according to its first arrival P wave take-off angle.

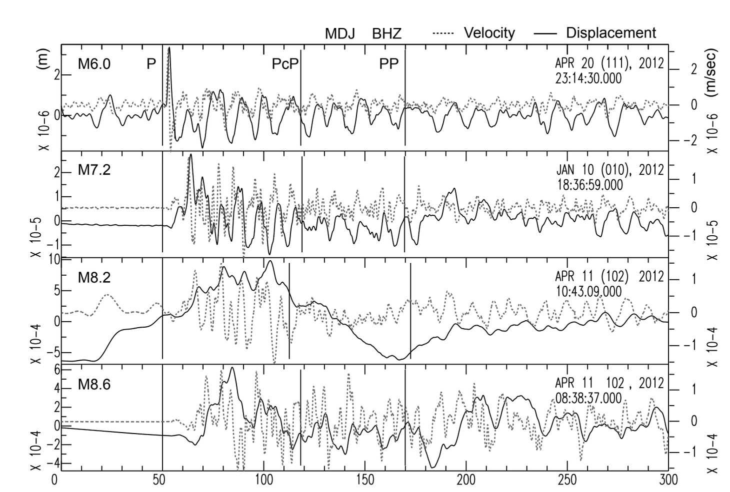

Figure 8

Figure 8. Teleseismic P-wave record for M6.0, M7.2, M8.2 and M8.6 earthquakes
Teleseismic P-wave vertical components for the M6.0 (aftershock), M7.2 (foreshock), M8.2 (aftershock) and M8.6 (main shock) earthquakes. Both velocity (dashed line) and displacement (solid line) records are displayed in the raw data, note the noise level in the M8.2 produced by the main event since it is an early aftershock (2 hours).

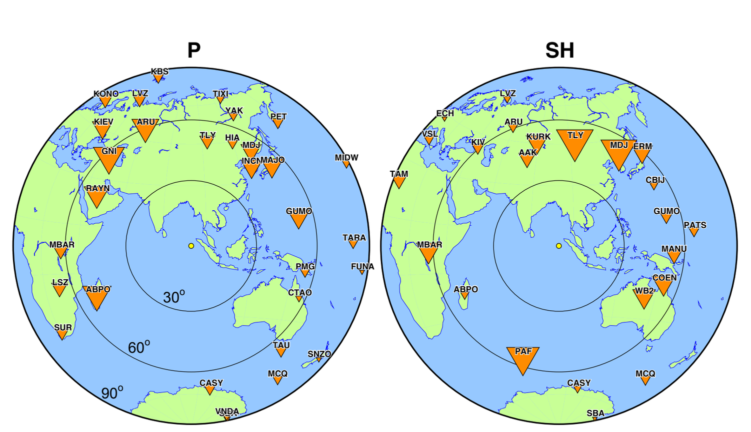

Figure 7

Figure 7. Teleseismic station map
Station distribution of teleseismic P and SH components used in the inversions. The size of triangle is proportional to the maximum displacement amplitude for each station. Here the triangle sizes for P-wave are amplified by 8 times to make them comparable with that for SH-wave. Note that the largest amplitude patterns are rotated by about 45° as predicted for a strike-slip event.

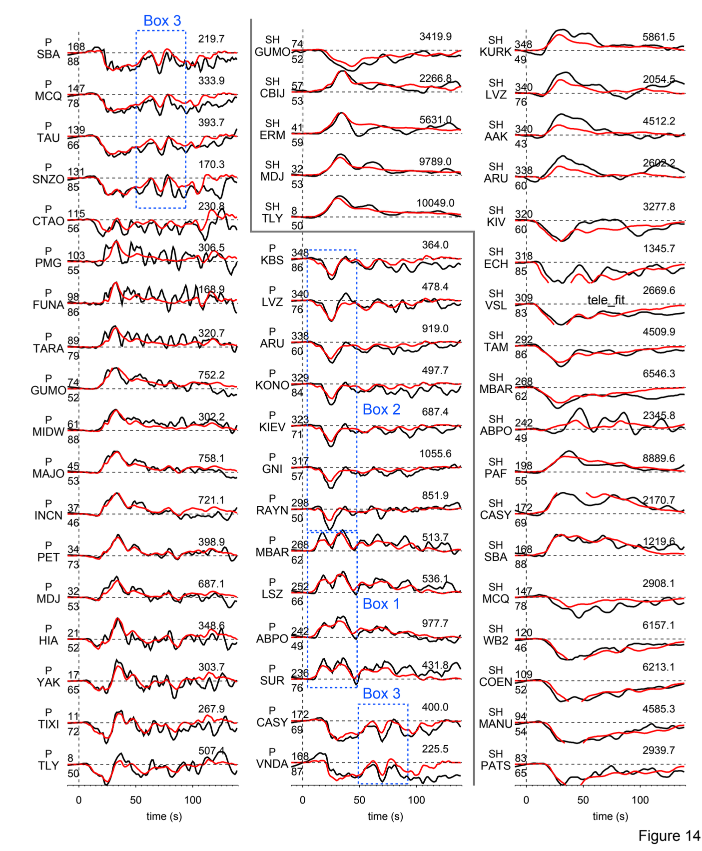

Figure 14

Figure 14. All teleseismic waveform fits
Teleseismic waveform fits for the joint inversion model, P waves and SH waves are separated by the gray line in the middle, see Fig.13 for detail of description. Stations at three azimuths groups are indicated by the dashed rectangles (Box1, Box2 and Box3) with representative stations shown in Fig.16.

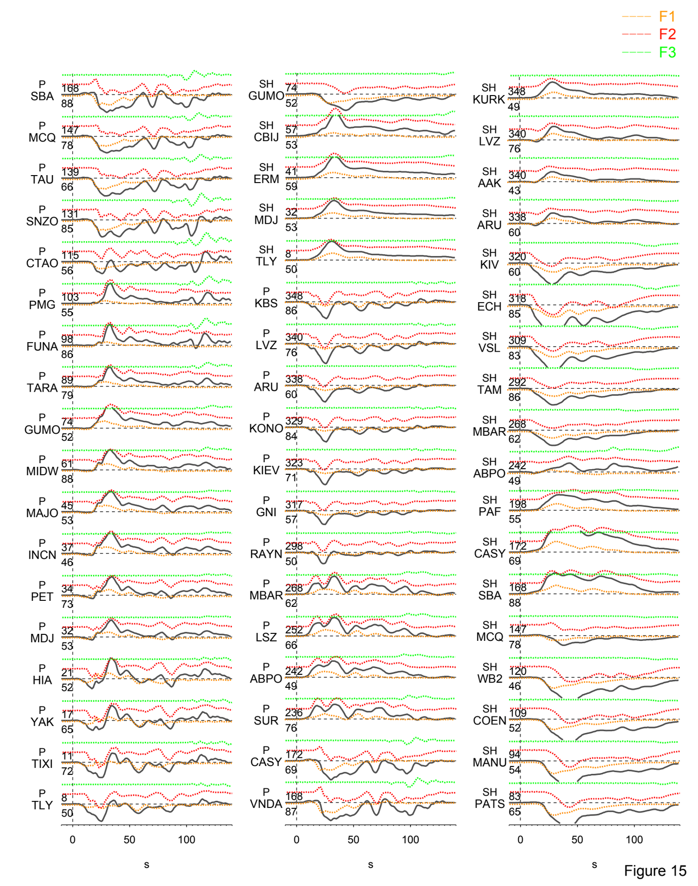

Figure 15

Figure 15. Separation of teleseismic waveform fits
Separation of teleseismic synthetics (gray) into the contribution of fault segment F1 (brown), F2 (red) and F3 (green).

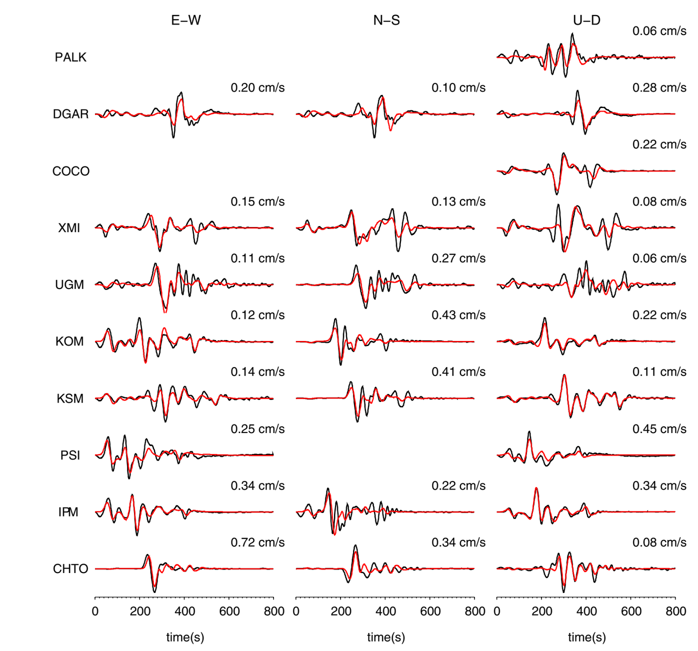

Figure 10

Figure 10. Regional waveform fits for the joint inversion model
Three components regional waveform fits for the joint inversion model, in which data is shown as black and synthetic as red. All waveforms are filtered to 50s and longer using the same filter as in Fig.2. Station names are indicated at the beginning, the number at the end of each pair is the maximum amplitude of data. The empty spaces are clipped components.

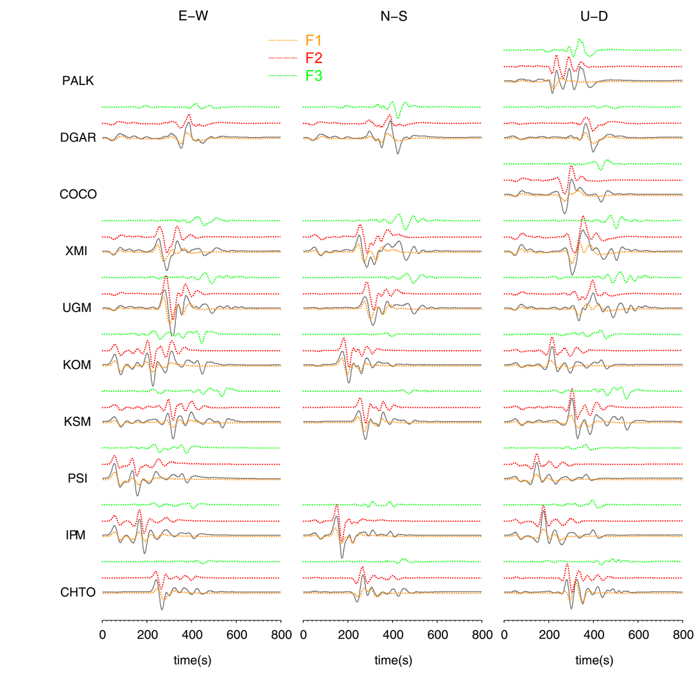

Figure 11

Figure 11. Separation of regional waveform fits
Separation of regional synthetic waveforms (grey) into the contribution of segment F1 (brown), F2 (red) and F3 (green). The gray trace is the sum.

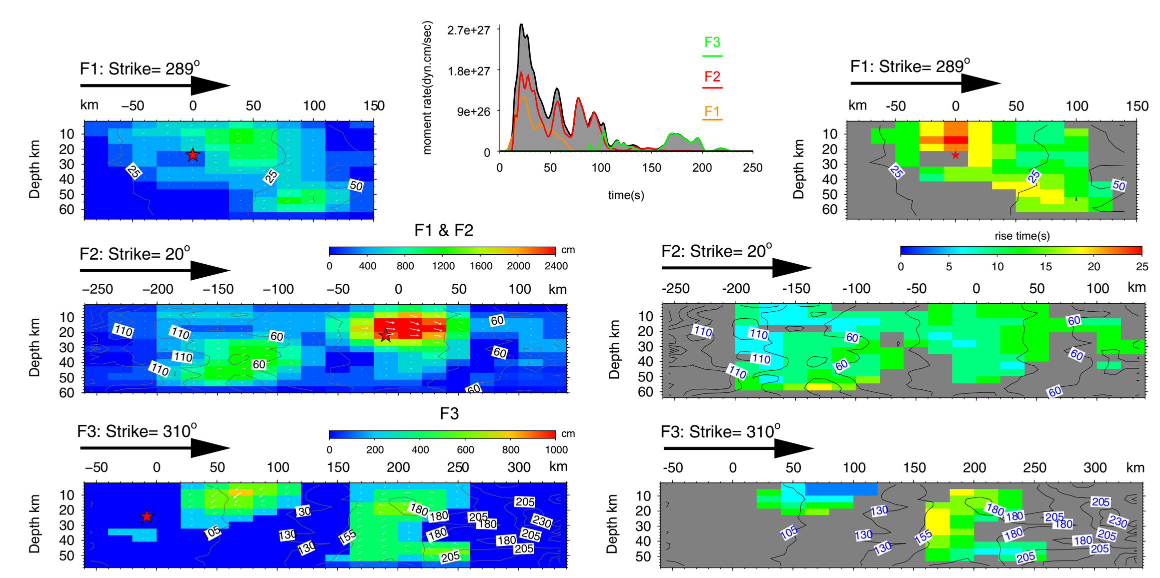

Figure 9

Figure 9. Slip model, moment-rate function, and rise time
Depth profiles of slip distribution (left), rise time (right) and moment rate (middle) of the joint inversion finite fault model. Slip and rise time are color coded, the contour lines are the rupture starting time relative to the epicenter origin time. Note that the interval of contour lines is 25s. Arrows in slip distribution indicate the rake angle. Contribution from different fault segment is shown in the moment rate function with the grey-shaded region indicating the total radiation-rate.

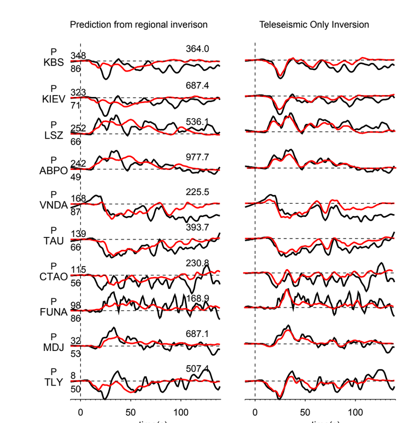

Figure 13

Figure 13. Representative teleseismic P-wave fits from regional only model and teleseismic only model
Selected teleseismic P-wave fits, (A) prediction from regional only inversion, (B) teleseismic only inversion. Data are displayed in black and synthetics are in red, station name is indicated at the beginning of each trace with epicenter distance in degree (lower) and azimuth (upper). Maximum amplitude of data in micro-meter is shown at the end of the seismogram.

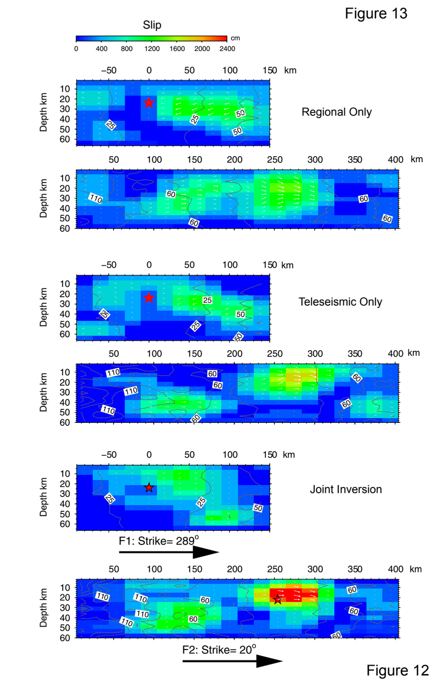

Figure 12

Figure 12. Slip model on F1 and F2 for regional only inversion, teleseismic only inversion and Joint inversion
Depth profiles of slip models for the regional only inversion (upper), teleseismic only inversion (middle) and joint inversion (lower). Here we only display segment F1 and F2.

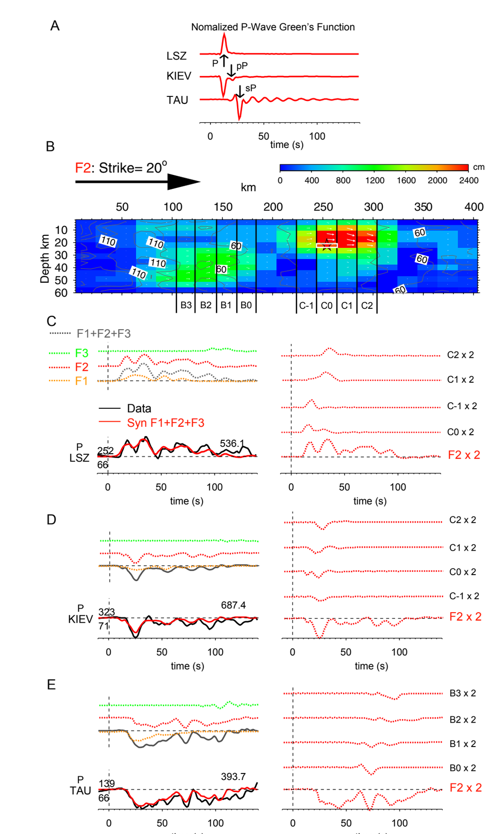

Figure 16

Figure 16. Representative teleseismic fits for stations at azimuth of 250°, 320° and 140°
Representative teleseismic stations (LSZ, KIEV, TAU) selected from three groups of stations as indicated in Fig.14. (A) Normalized Green's Functions for the three stations, direct P and ocean bottom reflection pP and sP phases are pointed out by arrows. The Green's Functions are computed by using unit slip on the subfault where the rupture on F2 was initiated, as shown in (B) by the small white rectangle. (B) Slip model on fault segment F2, see Fig.9 for detail of arrows and contours. The rupture on this fault is divided into different columns as shown. Corresponding synthetics are presented in C,D and E. (C) Lower left is the waveform fits of the joint inversion model at station LSZ, with decomposition into fault segment F1, F2 and F3 displayed on upper left. Right panel shows the contribution of columns C-1 to C2 compared with the total synthetics from F2. (D) and (E) are similar as (C) for station KIEV and TAU.

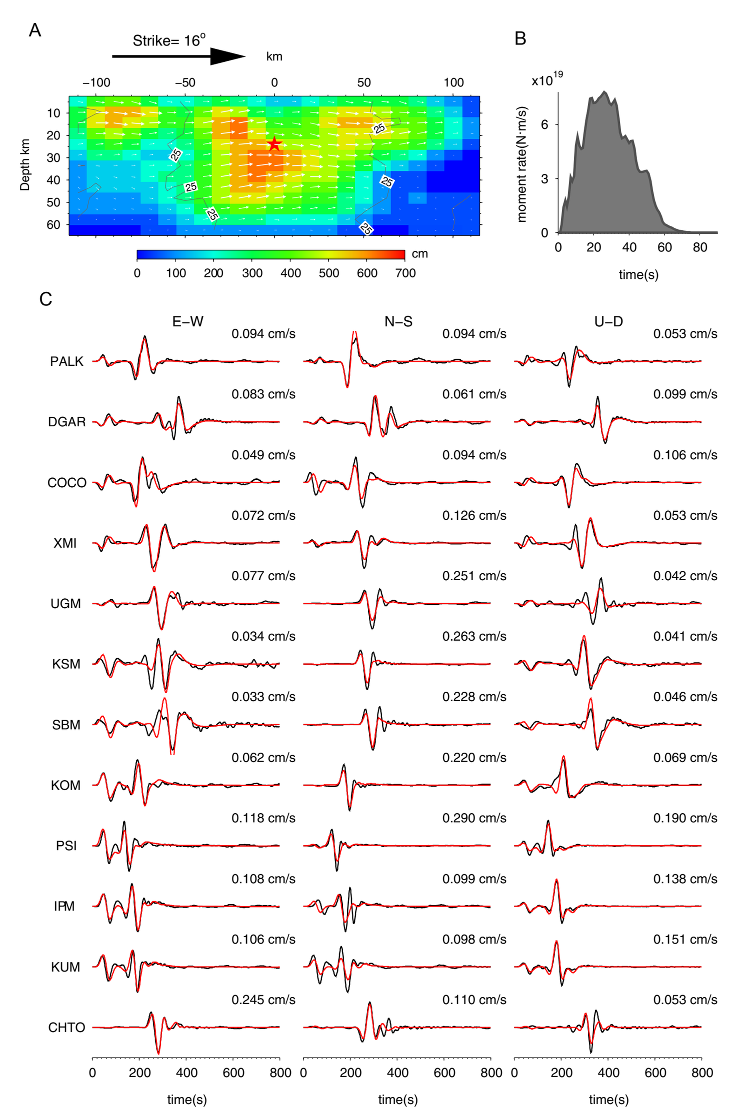

Figure 17

Figure 17. Slip model of M8.2 aftershock
(A) Depth profile of the slip model for the Mw8.2 aftershock; contour lines indicate the rupture starting time and the arrows show the rake angles. (B) Moment rate function. (C) Regional waveform fits with data in black and synthetics in red, all the seismograms are filtered to 50s and longer, see Fig.10 for detail of description.

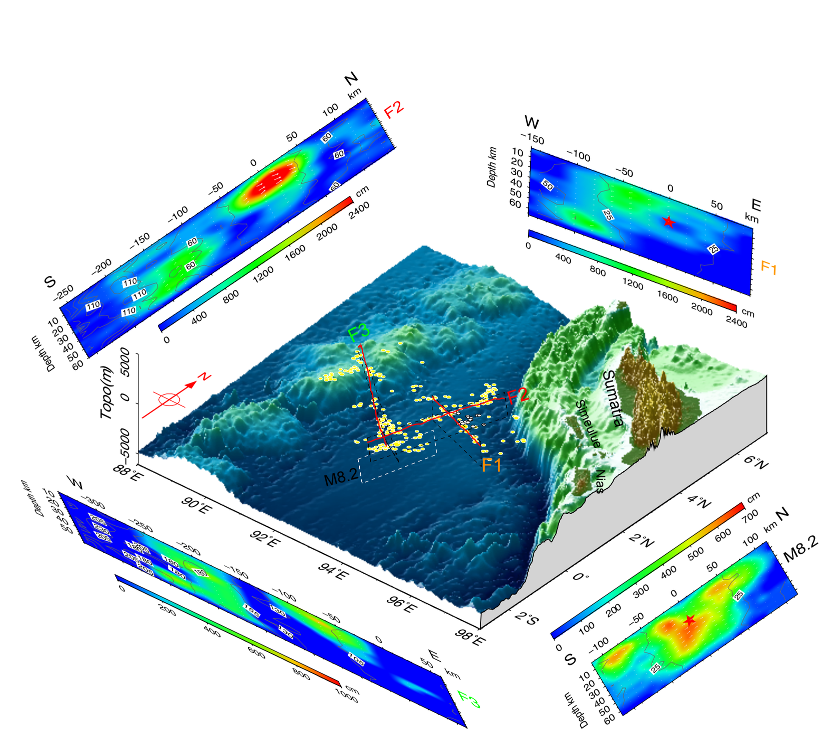

Figure 18

Figure 18. 3D view
The middle image is a 3D view of bathymetry and topography along with the schematic fault segments shown as rectangles. The red lines are the projection of the upper boundary of the fault plane of F1, F2 and F3 on the seafloor. Aftershocks are shown as yellow dots and the white dots are the foreshocks. Smoothed depth profiles of slip models of the 3 fault segments of the main shock and the Mw8.2 aftershock are shown on sides.

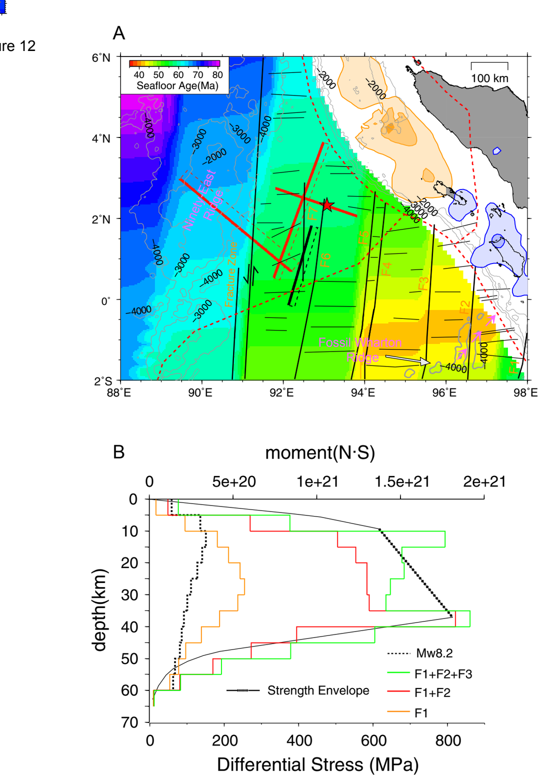

Figure 19

Figure 19. Fracture Zone, Seafloor Age and the Moment Depth Distribution
(A). Fracture zones (denoted as black lines and marked as F1 to F7) in this region are overlapping with the seafloor ages (Muller et al. 2008). The red rectangles are the map view of three fault planes used in the inversion and red star is the epicenter of the main event, the black rectangle is the fault plane used for the Mw8.2 aftershock. Note that the Fossil Wharton Ridge is subducting beneath the Sunda trench. Slip models of the 2004 (Mw9.2, yellow) and 2005 (Mw8.6, blue) megathrusts are shown as contours. The red dashed lines are the plate boundaries from (Bird 2003). (B). Depth distribution of moment release for both the mainshock and the aftershock, the contribution from different segments to the mainshock are shown in different colors. The black solid line is the strength envelope of the oceanic lithosphere, which is computed by the Byerlee's frictional sliding rule for the dry rock and rheology for olivine for the plastic flow (Kohlstedt et al. 1995).

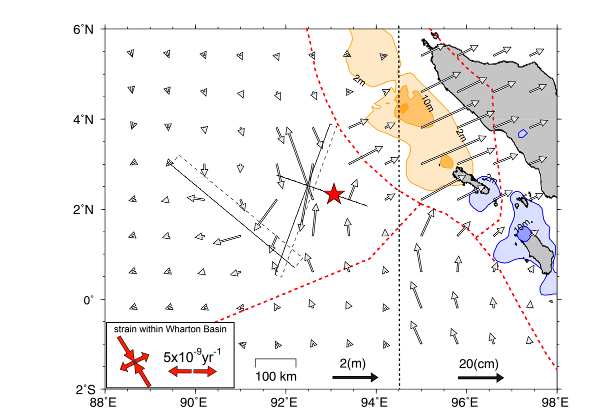

Figure 20

Figure 20. Prediction of static horizontal motion
The horizontal motion (vectors) predicted by the preferred slip model. Note the scale is different by a factor of 10 for region to the east and west of 94.5°E longitude line (dashed). The 2004 and 2005 megathrusts are shown as color contours. The red dashed lines are the plate boundaries from (Bird 2003). Fault planes used in the inversion are shown as rectangles. Note that the region has undergone a net comparison as indicated by the arrows. The red arrows in the low-left corner indicate the stain-rate in this region based on the model presented by (Delescluse & Chamot-Rooke 2007).

Conclusion

1. The main shock ruptured at least 3 fault segments (F1, F2 and F3) and the rupture delay between F1 and F2 is 10s and the delay is 80s for the rupture between F1 and F3. The total moment of the earthquake is 1.3×1022N•m and the total duration is about 210s. The moment distribution on F1, F2 and F3 is 3.3×1021N•m, 8.0×1021N.m and 1.9×1021N•m, respectively.
2. Both the mainshock and the Mw8.2 aftershock show slip patches as deep as 50km, and the largest co-seismic slip for the main event is up to 24m and is located on F2 near the intersection of F1 and F2. The estimated stress drop ranges from 10MPa~30MPa for the mainshock and is about 10MPa for the Mw8.2 aftershock.
3. This earthquake sequence has re-activated the NNE-SSW oriented fracture zones in the Wharton Basin and some ENE-WSW oriented faults included a segment which cuts across the Ninety-East Ridge.
4. This earthquake sequence is part of the diffuse deformation zone between the Indian and the Australian plates.
5. This earthquake sequence was probably triggered by static stress change induced by the Mw 9.2 great Sumatra earthquake of 2004.